Available online at www.sciencedirect.com
SCIENCE DIRECT®
Biochemical and Biophysical Research Communications 303 (2003) 223–229
BBRC
www.elsevier.com/locate/ybbrc

Characterization of aldehyde ferredoxin oxidoreductase gene defective mutant in *Magnetospirillum magneticum* AMB-1

Aris Tri Wahyudi, Haruko Takeyama, Yoshiko Okamura, Yorikane Fukuda, and Tadashi Matsunaga*

Department of Biotechnology, Tokyo University of Agriculture and Technology, 2-24-16 Naka-Cho, Koganei, Tokyo 184-8588, Japan

Received 17 February 2003

Abstract

A non-magnetic mutant of *Magnetospirillum magneticum* AMB-1, designated as NMA21, was generated by mini-Tn5 transposon mutagenesis to identify genes involved in bacterial magnetic particle (BMP) synthesis. Alignment of the DNA sequences flanking the transposon allowed the isolation of an open reading frame (ORF2) within an operon consisting of five genes. The amino acid sequence of ORF2 showed homology with tungsten-containing aldehyde ferredoxin oxidoreductase (AOR) from *Pyrococcus furiosus* (48% identity and 64% similarity), which functions for aldehyde oxidation. AOR was found to be expressed under microaerobic conditions and localized in the cytoplasm of AMB-1. Iron uptake and growth of NMA21 were lower than wild type. Transmission electron microscopy (TEM) of NMA21 revealed that no BMPs were completely synthesized, but polyhydroxybutyrate (PHB)-like granules were persistently produced. These results indicate that AOR may contribute to ferric iron reduction during BMP synthesis in *M. magneticum* AMB-1 under microaerobic respiration.

Keywords: *Magnetospirillum magneticum* AMB-1; Bacterial magnetic particle; Aldehyde ferredoxin oxidoreductase; Non-magnetic mutant

Magnetic bacteria synthesize intracellular membrane bound magnetic particles [1,2] of either an iron oxide, magnetite (Fe_3O_4) [2,3], or iron sulfide, greigite (Fe_3S_4) [4] which are postulated to confer biological advantage to the bacterium by moving along oxygen and iron gradients through the earth's geomagnetic field lines. Formation of this structure is achieved by a mineralization process with control over the accumulation of iron and the deposition of the mineral particle in the cell [5].

Since the discovery of magnetic bacteria in 1975 [6], only a few magnetic bacterial strains can be axenically cultivated in laboratory conditions. These include *Magnetospirillum magnetotacticum* MS-1 [7], *Magnetospirillum gryphiswaldense* [8], and *Magnetospirillum magneticum* AMB-1 [9]. These strains are usually used as model system for the analysis of bacterial magnetic particle (BMP) synthesis. The ability of *M. magneticum* AMB-1 to grow under both microaerobic and aerobic conditions in liquid or solid media [10] makes this bacterium amenable for genetic manipulations. This facilitates the elucidation of BMP synthesis from the gene level.

Several processes are involved in BMP synthesis, such as: (1) iron flux including iron uptake into cell and transport into vesicle (magnetosome) accompanied by redox reaction, (2) vesicle formation by invagination of cytoplasmic membrane, (3) magnetite crystallization in the vesicle, and (4) energy/proton flux with respiration. In the study of molecular analysis using *M. magneticum* AMB-1, several genes/proteins are demonstrated to be involved in the above processes. The MagA protein localized in BMP membrane functions for the iron transport across the BMP membrane [11]. Mms16 protein specific to BMP membrane has a GTPase activity, which primed the invagination of the cytoplasmic membrane for the formation of the BMP membrane [12]. The MpsA protein having homology with acyl-CoA carboxylase (transferase) and with acyl-CoA binding motif functioned as mediator for BMP

* Corresponding author. Fax: +81-42-385-7713.
E-mail address: tmatsuna@cc.tuat.ac.jp (T. Matsunaga).

0006-291X/03/$ - see front matter © 2003 Elsevier Science (USA). All rights reserved.
doi:10.1016/S0006-291X(03)00303-6

membrane invagination [13]. Furthermore, Mms6 protein isolated from BMP membrane was shown to function for the crystallization of ferric and ferrous ions under anaerobic conditions [14]. In *M. magneticum* AMB-1, iron reduction through quinone in the respiratory chain was demonstrated to be involved in BMP synthesis [15]. However, there are still no genetic studies related to this process.

Previously, non-magnetic mutants were generated by introduction of transposon mini-Tn5 into the genome of *M. magneticum* AMB-1 [16]. In this study, the genomic region interrupted by mini-Tn5 and its upstream and downstream sequences was analyzed. Cell growth and iron uptake of a non-magnetic mutant, NMA21, defective in aldehyde ferredoxin oxidoreductase gene were investigated.

Materials and methods

Bacterial strains, plasmids, and culture conditions. The bacterial strains and plasmids used in this study and their relevant characteristics are described in Table 1. *M. magneticum* AMB-1 (ATCC 700264) was routinely cultured microaerobically in magnetic spirillum growth medium (MSGM) at 25 °C [7]. A non-magnetic mutant of AMB-1, NMA21, was microaerobically cultured in MSGM supplemented with kanamycin (5 μg/ml), whereas *M. magneticum* AMB-1 carrying pUMP-AOR21 (see below) was cultured in MSGM supplemented with ampicillin (5 μg/ml). *Escherichia coli* DH5α was routinely cultured in Luria broth (LB) (tryptone 5.0 g/l, NaCl 10 g/l, and yeast extract 5.0 g/l) at 37 °C.

Isolation of flanking DNA and sequence analysis. Genomic DNA fragments flanking the transposon from NMA21 were isolated by inverse polymerase chain reaction (inverse PCR), purified using Gene Clean III Kit (Bio-101, Carlsbad, CA, USA), subsequently sub-cloned in pGEM-T Easy (Promega, Madison, WI, USA), and transformed into *E. coli* DH5α by electroporation. The recombinant plasmid was extracted from *E. coli* by Qiaprep Miniprep (Qiagen, Gmbh, Germany) and sequenced using an automatic DNA sequencer ABI 377 (Perkin–Elmer, USA). The DNA sequence was subsequently aligned against the whole genome sequence of *M. magneticum* AMB-1 [17]. The BLAST program [18] against the protein database was used for homologous searches of open reading frames (ORFs). A computer software package, Lasergene (DNASTAR, Madison, WI, USA), was used for DNA and protein sequence analysis.

Plasmid construction for gene expression. A gene cluster (Fig. 1A) identified through alignment of flanking DNA from NMA21 genome against the whole genome sequence of AMB-1 was analyzed. ORF1 and ORF2 were amplified by PCR using two oligonucleotide primers, primer 1: 5′-GGG ACT AGT TCT AGA ATG CAG AAA TCA TTG CTC-3′ and primer 2: 5′-GGG ACT AGT GGA TCC TCA GTG GTG GTG GTG GTG GTG GGC CAG TTG CAG GCG CTT-3′ (underlined DNA sequence indicates 6× Histag). PCR was performed with the following conditions. The 50 μl PCR mixture (LA Taq, Takara, Tokyo, Japan) contained 100 ng of *M. magneticum* AMB-1 genomic DNA. The temperature program for PCR was one cycle of 3 min at 95 °C, 30 cycles at 95 °C for 1 min, 1 min at 60 °C, and 1 min at 72 °C, and one cycle for 10 min at 72 °C. The amplified fragment was purified and sub-cloned into pCR2.1 (Invitrogen, Carlsbad, CA, USA), designated pCR2.1-ORF1-2, and subsequently cloned into pUMP16 [19] at the site of *Spe*I, to yield a recombinant plasmid pUMP-AOR21. This plasmid was introduced into *M. magneticum* AMB-1 by electroporation [20] and the transformant was cultured in MSGM containing ampicillin (5 μg/ml).

SDS–PAGE and Western blot analysis. The *M. magneticum* AMB-1 transformant carrying pUMP-AOR21 was microaerobically cultured to stationary phase with MSGM containing 5 μg/ml ampicillin at 25 °C. Cell fractionation was done according to the method described by Matsunaga et al. [13]. The AOR–histag fusion protein in the cellular membrane, cytoplasm, and BMP membrane fractions of recombinant AMB-1 (pUMP-AOR21) were determined by sodium dodecyl sulfate–polyacrylamide gel electrophoresis (SDS–PAGE) and Western blot.

Fractions of BMP membrane, cell membrane, and cytoplasm were mixed with 2× sample buffer and denatured by boiling for 5 min. The samples were subjected to SDS–PAGE using 12.5% (w/v) acrylamide gel and stained with silver stain II kit (Wako Chemical Industries, Osaka, Japan). For Western blotting, polyacrylamide gel was blotted onto an Immobilon-P polyvinylidene difluoride (PVDF) membrane (Millipore) by electroblotting and stained with monoclonal mouse anti-histag antibody (Qiagen, GmbH, Germany) at 1:5000 dilution. A secondary goat anti-mouse IgG antibody conjugated to alkaline phosphatase (Zymed Laboratories) was used for imaging.

Transmission electron microscopy (TEM). NMA21 from each growth phase was observed under light microscope (Olympus BH2, Tokyo, Japan) and a samarium-cobalt magnet was moved in different

Table 1
Bacterial strains and plasmids used in this study

Strain or plasmid	Relevant characteristics	Source or reference
Escherichia coli strain		
DH5α	*sup*E44Δ*lac*U169 (Φ80 *lac*ZΔM15), *rec*A1*hsd*R17, *end*A1*gyr*A96, *thi*-1 *rel*A1	[35]
M. magneticum strains		
AMB-1	Wild type, magnetic	[9]
AMB-1 (AOR21)	Wild type carrying plasmid (pUMP-AOR21), magnetic, ApR	This study
NMA21	Non-magnetic mutant, mini-Tn5Kml, KmR	[16]
Plasmids		
pGEM-TEasy	PCR cloning vector, 2.9 kb, ApR	Promega
pCR2.1	PCR cloning vector, 3.9 kb, ApR, KmR	Invitrogen
pUMG	3.7 kb pMGT/*Bam*HI cloned in pUC18, ApR, expression vector	[20]
pUMP16	0.6 kb DNA/*Eco*RI containing promoter *mms*16 cloned in pUMG, ApR	[19]
pCR2.1-ORFl-2	2.4 kb PCR product of ORF1 and ORF2 cloned in pCR2.1, ApR, and KmR	This study
pUMP-AOR21	2.4 kb ORF1 + ORF2-Histag/*Spe*I cloned in pUMP16, ApR	This study

ApR, amphicillin resistance; KmR, kanamycin resistance.

directions near the glass slide to determine the cell's magnetic response. For electron microscopic observation, 2 μl culture of NMA21 (approx. 1×10^8 cells/ml) from each growth phase was placed onto copper electron microscopy grid and allowed to settle for 1–2 h. Excess liquid was removed with a piece of filter paper and stained with 2% phosphotungstic acid for 15 min. The grid was air dried and observed by TEM (model H-700H, Hitachi, Japan).

Measurement of cell growth. To measure the cell growth of NMA21 and *M. magneticum* AMB-1, cells were cultured in MSGM under microaerobic and aerobic conditions with shaking at 100 rpm at 25 °C, until stationary phase. Initial cell concentration inoculated to the medium was approximately 1×10^5 cells/ml. Cell growth was measured by counting cells using a hemocytometer under the light microscope (Olympus BH2, Tokyo, Japan).

Measurement of iron uptake. Stationary-phase of wild type *M. magneticum* AMB-1 and NMA21 microaerobically cultivated in MSGM containing 33 μM ferric ion was harvested by centrifugation, washed with iron-free MSGM, and resuspended in MSGM containing 330 μM of ferric iron with an initial cell concentration of 1×10^9 cells/ml. The cell cultures were incubated under microaerobic conditions. Iron uptake ability of the cells was monitored by measuring the decrease of iron concentration in the medium. Iron concentration was measured using ferrozine [21,22] from samples aliquoted at different times.

Results

Genetic organization of a gene interrupted by transposon

Inverse PCR amplification of upstream and downstream sequence of the DNA flanking the transposon from NMA21 allowed the isolation of a 823 bp DNA sequence. To characterize this locus, we obtained its upstream and downstream sequences through alignment against the genome sequence of *M. magneticum* AMB-1. An ORF directly interrupted by transposon, ORF2 (Fig. 1A), consisting of 1851 bp was obtained. Target sequence of the transposon was CTC CTA CAC located at 1399–1407 bp position from the start codon (ATG). Putative ribosomal binding site (RBS) was found at 8 bp position upstream of the start codon. A putative promoter sequence (Fig. 1B) was only found upstream of the start codon of ORF1–ORF5. Therefore, ORF1–ORF5 may be organized in an operon.

Homology analysis of amino acid sequence deduced from ORFs

The results of homology analysis of amino acid sequence deduced from ORFs are shown in Table 2. ORF1 has high homology with the putative oxidoreductase Fe–S subunit from *Pyrococcus furiosus* DSM 3638 (45% identity, 57% similarity), with a predicted molecular mass of 17.3 kDa. Analysis of this sequence revealed that it contains four 4Fe–4S motifs of ferredoxin, LLIQPAKCTGCR, WCLQACPVDAIG, NDNICVGCKVCT, and ACAKACPTGAIT. Therefore, the protein encoded by ORF1 may be ferredoxin which has functions as electron transfer during oxidation/reduction.

ORF2 encodes a protein of 617 amino acids with a molecular mass of 66.3 kDa and has a high degree of homology with tungsten-containing aldehyde ferredoxine oxidoreductase (AOR) from *P. furiosus* (48% identity and 64% similarity) (Table 2). Further analysis indicated that the sequence contains consensus sequences for AOR. Alignments of amino acid sequences

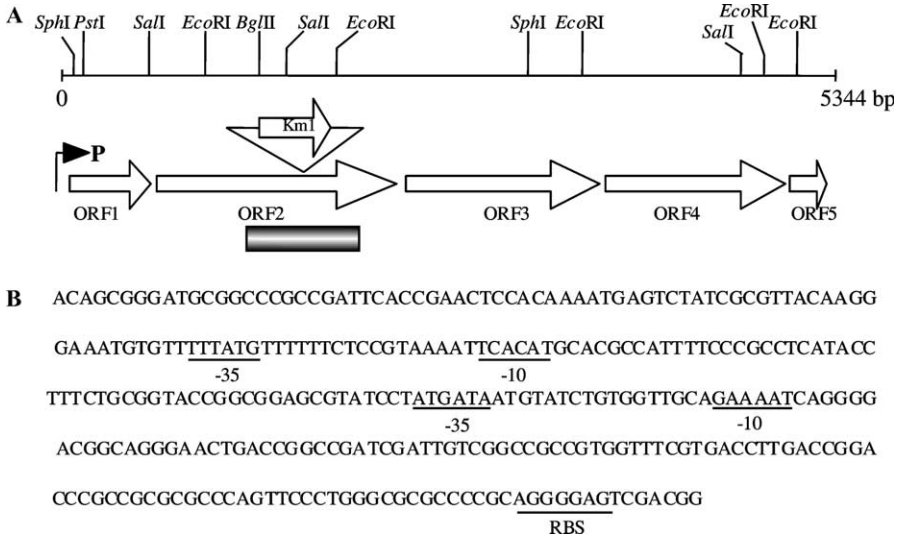

Fig. 1. (A) Physical map of a gene cluster containing the genes involved in BMP synthesis organized in an operon consisting of five ORFs. Position of restriction sites is also shown above the map. Arrow with P indicates the position of putative promoter and direction of transcription. Triangle with arrow Km1 indicates the location of mini-Tn5 transposon insertion and direction of its transcription. ORF, open reading frame; Km1, kanamycin resistance gene. Black box under the ORF2 indicates DNA flanking transposon amplified by inverse PCR and sequenced. (B) The DNA sequence containing putative promoter upstream of ORF1. RBS, ribosomal binding site.

Table 2
Homologous searches of an operon involved in bacterial magnetic particle synthesis

ORF	Size (bp)	Amino acid residue	Mol. mass (kDa)	Homologous protein	Protein Accession No.	Id/Sim (%)	Microorganism
1	480	160	17.3	Oxidoreductase Fe–S subunit	AAL81603	45/57	*Pyrococcus furiosus*
2	1851	617	66.3	Tungsten-containing aldehyde ferredoxin oxidoreductase	Q51739	48/64	*Pyrococcus furiosus*
3	1302	434	46.1	NADH oxidase	AAD 35480	31/47	*Thermotoga maritima*
4	1251	417	44.7	Assimilatory nitrate reductase electron transfer subunit	P42433	27/47	*Bacillus subtilis*
5	246	82	8.3	Molybdenum cofactor biosynthesis protein D/E	E75252	35/55	*Deinococcus radiodurans*

Id, identity; Sim, similarity.

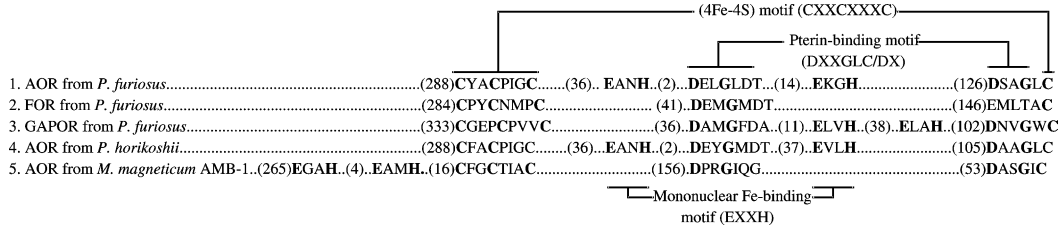

Fig. 2. Alignments of the cofactor-binding motifs of AOR, FOR, GAPOR from *P. furious* (1–3), AOR from *P. horikoshii* (4), and putative AOR from *M. magneticum* AMB-1 (5). The numbers in parentheses indicate the numbers of residues between the indicated motifs.

of: (1) AOR, (2) formaldehyde ferredoxin oxidoreductase (FOR) and (3) glyceraldehyde-3-phosphate ferredoxin oxidoreductase (GAPOR) from *P. furiosus* [23], (4) AOR from *P. horikoshii*, and (5) AOR from AMB-1 are shown in Fig. 2. AOR from AMB-1 contains two pterin-binding motifs (DPRGIQ and DASGIC) and cystein-cluster motif CXXCXXXC (CFGCTIAC) similar to *P. furiosus* and *P. horikoshii*, indicating that it contains one [4Fe–4S] cluster and a mononuclear tungstobispterin cofactor [23]. AOR from AMB-1 also contains two EXXH motifs (EGAH and EAMH) which coordinate a mononuclear metal site, most likely iron, which bridges the two subunits in AORs from *P. furiosus* and *P. horikoshii*. However, in AMB-1, these motifs are in different locations as those of AORs from *P. furiosus* and *P. horikoshii*. AORs from AMB-1 may lack the subunit-bridging metal ion found in AORs of *P. furiosus* and *P. horikoshii*. Molecular phylogenetic analysis showed that this AOR is classified into the AOR cluster among the AOR family containing AOR, FOR, and GAPOR. Even though the EXXH motifs are in different locations, this enzyme may have similar function to the AOR family such as GAPOR (Fig. 2).

Open reading frames 3 and 4 encode proteins of 434 and 417 amino acids with molecular masses of 46.1 and 44.7 kDa, respectively. These amino acid sequences showed homology with NADH oxidase from *Thermotoga maritima* (31% identity and 47% similarity), which is a major component of electron transport pathway [24] and assimilatory nitrate reductase electron transfer subunit, NasB [25], from *Bacillus subtilis* (27% identity and 47% similarity), respectively (Table 2).

Open reading frame 5 encodes a protein of 82 amino acids with a molecular mass of 8.3 kDa and has homology with the molybdenum cofactor biosynthesis protein D/E from *Deinococcus radiodurans* (35% identity and 55% similarity).

Expression and localization of AOR in M. magneticum AMB-1

The recombinant plasmid pUMP-AOR21 containing ferredoxin gene (ORF1) and AOR gene (ORF2) with histag was transformed and expressed in *M. magneticum* AMB-1. Western blot analysis showed that the AOR–histag fusion protein (68 kDa) was expressed in the AMB-1 recombinant. Analysis by SDS–PAGE and Western blot of BMP membrane, cell membrane, and cytoplasmic fractions indicated that the AOR–histag fusion protein was detected in the cytoplasmic fraction and some amount of this protein was expressed in the cell membrane (Fig. 3). There was no AOR–histag fusion protein that was detected on the BMP membrane fraction. These results suggest that the AOR protein in *M. magneticum* AMB-1 is mainly localized in the cytoplasm.

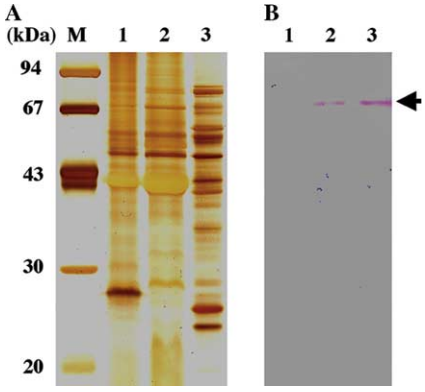

Fig. 3. (A) Silver-stained kit of sodium dodecyl sulfate–polyacrylamide gel electrophoresis of protein profile. (B) Western blot analysis of proteins fractionated from *M. magneticum* AMB-1 recombinant carrying pUMP-AOR21. Approximately 40 μg of protein from each fraction was applied. Lane M, molecular weight marker protein. Lane 1, BMP membrane fraction. Lane 2, cell membrane solubilysate. Lane 3, cytoplasmic fraction. Arrowhead indicates AOR–histag fusion protein expressed in recombinant AMB-1.

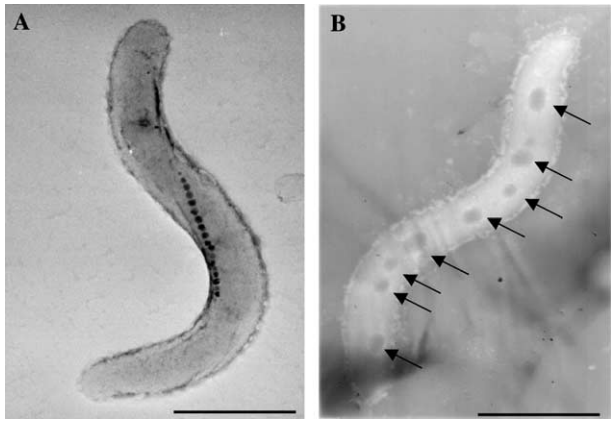

Fig. 4. Transmission electron micrograph of *M. magneticum* AMB-1. (A) Wild type AMB-1 with BMP in chain along the length of the cell. (B) Non-magnetic mutant NMA21 with new structures formed in the cell as indicated by arrowhead. Scale bar = 1 μm.

Electron microscopy of non-magnetic mutant NMA21 cells

Observation of the non-magnetic mutant NMA21 cells under light microscopy showed that cells did not respond to magnetic fields. This indicated that bacterial magnetic particles (BMPs) were not synthesized. To confirm this result, we observed NMA21 cells by TEM and it revealed that the cells did not contain the typical highly organized BMPs aligned in chains observed in wild type. Instead, new structures were persistent from lag to late stationary phase of the mutant (Fig. 4). Energy dispersive X-ray analysis of the structures revealed that it was not composed of magnetite like those found in wild-type (data not shown). The new structures may possibly be polyhydroxybutyrate (PHB)-like granules. Balkwill et al. [26] have also reported in a spontaneous non-magnetic mutant of *M. magnetotacticum* MS-1 producing a large amount of PHB granules observed by TEM.

Cell growth of non-magnetic mutant NMA21

As shown in Fig. 5, the growth curves of NMA21 and AMB-1 cells cultured in MSGM under microaerobic and aerobic conditions were compared. Initial cell concentration inoculated was at approximately 1.0×10^5 cells/ml. Under aerobic conditions, final cell concentrations of AMB-1 and NMA21 were similar, i.e., approximately 6.1×10^8 cells/ml (Fig. 5A). By contrast, higher final cell concentration was obtained in wild type than that in NMA21 under microaerobic conditions (Fig. 5B).

Iron uptake ability of NMA21

Ferric iron uptake ability of wild type AMB-1 and NMA21 under microaerobic conditions was indicated

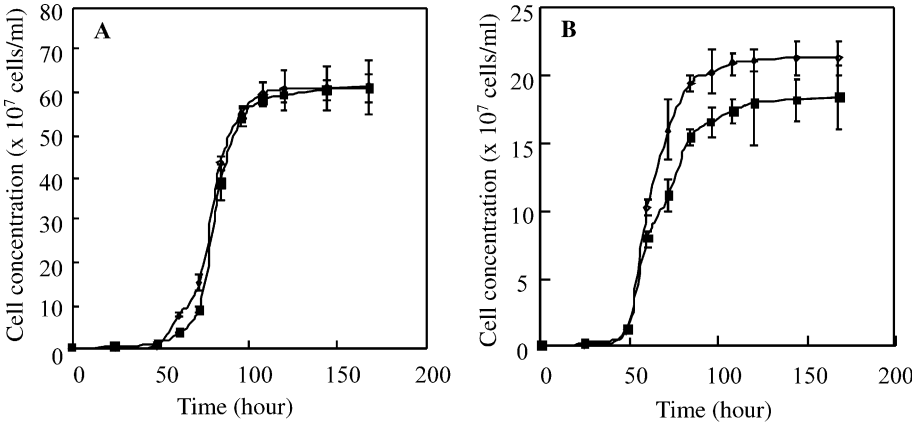

Fig. 5. Growth curves of *M. magneticum* AMB-1 wild type (◆) and NMA21 (■) cultured at 25 °C under aerobic (A) and microaerobic (B) conditions. Initial cell concentration inoculated to the medium is 1.0×10^5 cells/ml.

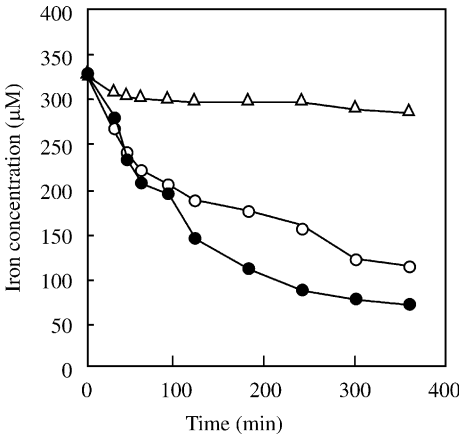

Fig. 6. Iron uptake by *M. magneticum* AMB-1 wild type at 25 °C (●), 4 °C (△) and mutant NMA21 at 25 °C (○) under microaerobic conditions.

by the decrease of iron concentration in the medium (Fig. 6). Iron concentration was relatively constant when the wild type AMB-1 culture was incubated at 4 °C, indicating that absorption and precipitation of iron by the cell did not occur. The decrease of iron concentration in the medium was due to the positive iron uptake by the bacterial cells. The ferric iron uptake of NMA21 cells was slightly inhibited by the mutation in AOR operon.

Discussion

In this study, ORF2 encoding AOR was directly interrupted by mini-Tn5 transposon rendered *M. magneticum* AMB-1 defective in complete BMP synthesis. Similar AOR genes were also found in other bacteria such as *Eubacterium acidaminophilum*, *P. horikoshii*, *Thermoplasma volcanium*, *Archaeoglobus fulgidus*, and *Methanosarcina mazei*. Sub-cellular analyses of recombinant AOR protein in AMB-1 indicated that it was mainly localized in the cytoplasm. Such localization is similar to that in *Thermococcus* ES-1 where AOR protein is 95% localized in the cytoplasm [27].

Analysis of the AOR operon in AMB-1 indicated that five genes are organized in a cluster, as an operon (Fig. 1) and can function as one unit for BMP synthesis under the same control. Molybdenum cofactor biosynthesis protein encoded by ORF5 involved in the biosynthesis of molybdopterin (MPT) is required for the maturation of AOR as a molybdenum cofactor. MPT is a substituted pterin derivative containing a 4-carbon side chain with a dithiolene group and mononuclear molybdenum or tungsten center [28]. Biosynthesis of MPT is initiated by guanosine triphosphate (GTP) in which the ring opening led to the labile precursor Z which is sulfurylated and converted to MPT by MPT synthase or MPT biosynthesis protein. Since there are several operons for MPT biosynthesis in AMB-1 genome (unpublished data), this independent constitution in AOR operon could attribute to initiate the in situ biosynthesis of MPT.

AOR functions for the reversible oxidation/reduction of aldehyde to carboxylic acid, with ferredoxin being reduced [29,30]. Electron from this reaction usually flows to NAD(P) or NAD(P)H. These reactions usually occur on the cell membrane [31] and the electron flows to electron transport system [32]. Therefore, proteins encoded by ORF3 (NADH oxidase) and ORF4 (assimilatory nitrate reductase electron transfer subunit) may have functions as electron transfer from ferredoxin encoded by ORF1 during oxidation/reduction and subsequently the electron could be used to reduce ferric to ferrous iron used for BMP synthesis. Some organisms apparently use respiratory chain components for iron reduction [33]. Both ORF3 and ORF4 are two helix transmembrane protein and they could be localized to cytoplasmic membrane. Localization analysis for recombinant AOR in AMB-1 showed slight existence on cytoplasmic membrane because of the interaction between AOR and those proteins on cytoplasmic membrane.

Energy/proton flux with respiration is involved in BMP synthesis. *Magnetospirillum* spp. are capable of nitrate respiration. Our previous study on the relationship between respiration and iron reduction in the facultative microaerobe *M. magneticum* AMB-1 showed that both potassium cyanate, known as an inhibitor for oxygen respiration, and 2-heptyl-4-hydroxyquinoline N-oxide (HQNQ), inhibitor for nitrate reduction respiration, did not inhibit the reduction of ferric ion. By contrast, when an inhibitor for electron transport to quinone, dicumarol, was used, ferric reduction, and BMP synthesis were inhibited. These data showed that electron transport required for BMP synthesis might be branched at quinone in respiratory chain in AMB-1 [15]. On the other hand, in strict microaerobe *M. magnetotacticum* MS-1, ferric reduction by electron branched at cytochrome *c* oxidase was demonstrated [34].

When NMA21 cells were cultured under aerobic conditions, the cell growth was similar to the AMB-1 wild type. In contrast, under microaerobic conditions the cell growth of NMA21 was repressed (Figs. 5A and B). These results indicate that AOR complex is not required under aerobic conditions, but under microaerobic conditions growth inhibition may be caused by unbalanced iron accumulation without BMP synthesis since non-magnetic mutant still uptakes enormous ferric ion. Furthermore, AOR links to the electron flux in respiratory chain and therefore deactivation of AOR may also affect the cell growth.

Taken the data all together, it can be speculated that this operon may contribute to ferric iron reduction

during BMP synthesis under microaerobic respiration. Mutation within this operon in ORF2 generated cells lacking highly organized BMPs aligned in chains for the cell's magnetotactic response.

Acknowledgments

This work was supported in part by Grant-in-Aid for Scientific Research on Specially Promoted Research 13002005 from the Ministry of Education, Culture, Science, Sports and Technology of Japan.

References

[1] Y.A. Gorby, T.J. Beveridge, R.P. Blakemore, Characterization of the bacterial magnetosome membrane, J. Bacteriol. 170 (1988) 834–841.
[2] T. Matsunaga, Applications of bacterial magnets, Trends Biotechnol. 9 (1991) 91–95.
[3] D.A. Bazylinski, Anaerobic production of magnetite by a marine magnetotactic bacterium, Nature 334 (1988) 518–519.
[4] D.A. Bazylinski, B.R. Heywood, R.B. Frankel, Fe_3O_4 and Fe_3S_4 in a bacterium, Nature 366 (1993) 218.
[5] D. Schuler, R.B. Frankel, Bacterial magnetosomes: microbiology, biomineralization and biotechnological applications, Appl. Microbiol. Biotechnol. 52 (1999) 464–473.
[6] R.P. Blakemore, Magnetotactic bacteria, Science 190 (1975) 377–379.
[7] R.P. Blakemore, D. Maratea, R. Wolf, Isolation and pure culture of a fresh water magnetic spirillum in defined growth medium, J. Bacteriol. 140 (1979) 720–729.
[8] K.H. Schleifer, D. Schueler, S. Spring, M. Weizenegger, R. Amann, W. Ludwig, M. Kohler, The genus *Magnetospirillum*, gen. Nov., description of *Magnetospirillum gryphiswaldense* and transfer of *Aquaspirillum magnetotacticum* to *Magnetospirillum magnetotacticum*, comb. Nov, Syst. Appl. Microbiol. 14 (1991) 379–385.
[9] T. Matsunaga, T. Sakaguchi, F. Todokoro, Magnetite formation by a magnetic bacterium capable of growing aerobically, Appl. Microbiol. Biotechnol. 35 (1991) 651–655.
[10] T. Matsunaga, C. Nakamura, J.G. Burgess, K. Sode, Gene transfer in magnetic bacteria: transposon mutagenesis and cloning of genomic DNA fragments required for magnetite synthesis, J. Bacteriol. 174 (1992) 2748–2753.
[11] C. Nakamura, J.G. Burgess, K. Sode, T. Matsunaga, An iron-regulated gene, *mag* A, encoding an iron transport protein of *Magnetospirillum* sp. AMB-1, J. Biol. Chem. 270 (1995) 28392–28396.
[12] Y. Okamura, H. Takeyama, T. Matsunaga, A magnetosome-specific GTPase from the magnetic bacterium *Magnetospirillum magneticum* AMB-1, J. Biol. Chem. 276 (2001) 48183–48188.
[13] T. Matsunaga, N. Tsujimura, Y. Okamura, H. Takeyama, Cloning and characterization of a gene *mpsA* encoding a protein associated with intracellular magnetic particles from *Magnetospirillum* sp. Strain AMB-1, Biochem. Biophys. Res. Commun. 268 (2000) 932–937.
[14] A. Arakaki, J. Webb, T. Matsunaga, A novel protein tightly bound to bacterial magnetic particles in *Magnetospirillum magneticum* strain AMB-1, J. Biol. Chem. 278 (2003) 8745–8750.
[15] T. Matsunaga, N. Tsujimura, Respiratory inhibitor of a magnetic bacterium *Magnetospirillum* sp. AMB-1 capable of growing aerobically, Appl. Microbiol. Biotechnol. 39 (1993) 368–371.
[16] A.T. Wahyudi, H. Takeyama, T. Matsunaga, Isolation of *Magnetospirillum magneticum* AMB-1 mutants defective in bacterial magnetic particle synthesis by transposon mutagenesis, Appl. Biochem. Biotechnol. 91–93 (2001) 147–154.
[17] T. Matsunaga, et al., The complete genome sequence of the magnetic bacterium *Magnetospirillum magneticum* strain AMB-1, in preparation.
[18] S.F. Altchul, T.L. Madden, A.A. Scaffer, J. Zhang, Z. Zhang, W. Miller, D.J. Lipman, Gapped BLAST and PSI-BLAST: a new generation of protein database search programs, Nucleic Acids Res. 25 (1997) 3389–3402.
[19] T. Matsunaga, M. Takahashi, T. Yoshino, F. Kato, Y. Okamura, H. Takeyama, Surface display of estrogen receptor on bacterial magnetic particles using Mms16 protein as an anchor molecule, in preparation.
[20] Y. Okamura, H. Takeyama, T. Sekine, T. Sakaguchi, A.T. Wahyudi, R. Sato, S. Kamiya, T. Matsunaga, Characterization of a new cryptic plasmid pMGT from a magnetic bacterium *Magnetospirillum magneticum* and application to gene transfer for protein expression on bacterial magnetic particles, submitted.
[21] C. Nakamura, Y. Hotta, R.H. Thornhill, T. Matsunaga, Characterization of nonmagnetic mutant of *Magnetospirillum* sp. Strain AMB-1, J. Mar. Biotechnol. 3 (1995) 97–100.
[22] L.L. Stooky, Ferrozine—a new spectrophotometric reagent for iron, Anal. Chem. 42 (1970) 779–781.
[23] R. Roy, S. Mukund, G.J. Schut, D.M. Dunn, R. Weiss, W.W.W. Adams, Purification and molecular characterization of the tungsten-containing formaldehyde ferredoxin oxidoreductase from the hyperthermophilic archaeon *Pyrococcus furiosus*: the third of a putative five-member tungstoenzyme family, J. Bacteriol. 181 (1999) 1171–1180.
[24] D.M. Brown, J.A. Upcroft, M.R. Edwards, P. Upcroft, Anaerobic bacterial metabolism in the ancient eukaryote *Giardia duodenalis*, Int. J. Parasitol. 28 (1998) 149–164.
[25] H. Ogawa, E. Akagawa, K. Yamane, Z. Sun, M. Lacelle, P. Zuber, M.M. Nakano, The *nas*B operon and *nas*A gene are required for nitrate/nitrite assimilation in *Bacillus subtilis*, J. Bacteriol. 177 (1995) 1409–1413.
[26] D.L. Balkwill, D. Maratea, R.P. Blakemore, Ultrastructure of a magnetotactic spirillum, J. Bacteriol. 141 (1980) 1399–1408.
[27] J. Heider, K. Ma, W.W.W. Adams, Purification, characterization, and metabolic function of tungsten-containing aldehyde ferredoxin oxidoreductase from the hyperthermophilic and proteolytic archaeon *Thermococcuus* strain ES-1, J. Bacteriol. 177 (1995) 4757–4764.
[28] C. Kisker, H. Schindelin, D. Baas, J. Retey, R.U. Meckenstock, P.M.H. Kroneck, A structural comparison of molybdenum cofactor-containing enzymes, FEMS Microbiol. Lett. 22 (1999) 503–521.
[29] S. Mukund, W.W.W. Adams, The novel tungsten–iron–sulfur protein of the hyperthermophylic archaebacterium *Pyrococcus furiosus* is an aldehyde ferredoxin oxidoreductase: evidence for its participation in a unique glycolytic pathway, J. Biol. Chem. 266 (1991) 14208–14216.
[30] A. Kletzin, W.W.W. Adams, Tungsten in biological systems, FEMS Microbiol. Rev. 18 (1996) 5–63.
[31] J. Hugenholtz, L.G. Ljungdahl, Metabolism and energy generation in omoacetogenic clostridia, FEMS Microbiol. Rev. 87 (1990) 383–390.
[32] M.D. Kantika, S. Duprat, E. Cornillot, et al., Genome sequence and gene compaction of the eukaryote parasite *Encephalitozoon cuniculi*, Nature 414 (2001) 450–453.
[33] H.A. Dailey, J. Lascelles, Reduction of iron and synthesis of protoheme by *Spirillum itersonii* and other organisms, J. Bacteriol. 129 (1977) 815–820.
[34] K.A. Short, R.P. Blakemore, Iron respiration-driven proton translocation in aerobic bacteria, J. Bacteriol. 167 (1986) 729–731.
[35] J. Sambrook, D.W. Russell, Molecular Cloning: A Laboratory Manual, Cold Spring Harbor Laboratory Press, Cold Spring Harbor, New York, 2001.